

原 著 論 文

An approach for removing artifacts from resting state fMRI signals

Yul-Wan Sung and Seiji Ogawa

Kansei Fukushi Research Institute, Tohoku Fukushi University

Abstract

Resting state functional MRI (rsfMRI) is a promising method for investigating brain disorders because it is non-invasive and does not require task performance as in typical task-fMRI studies. Since rsfMRI first description, many studies on brain disorders have demonstrated its potential as a detection or diagnosis tool. However, most conclusions are based on group studies. Their application to individuals requires overcoming some challenges such as reducing physical and physiological noises. Several methods of noise reduction for rsfMRI have already been established but further noise reduction is required for an individual application of rsfMRI. Here we propose a new approach in which we restricted the MRI measurement environment to the MRI scanner and one subject, from which we generated a noise set that was subtracted from rsfMRI data acquired with the same MRI scanner or subject. The present preliminary study examined the validity of the proposed approach using data from a phantom model and a human subject. Noises from rsfMRI data were removed by regression of previously prepared noise signals. The resulting signal presented properties similar to band-pass filtered one, suggesting the efficacy of the approach. In the future, the approach potential will be assessed using with more human subjects.

Keywords : Resting state fMRI (rsfMRI), Regression, Physical noise, Physiological noise, Intrinsic function

Introduction

Task-based functional MRI (tb-fMRI) has been used to map human brain functions. The tb-fMRI signal is measured while tasks related to a specific perception or cognition function are performed. In comparison with tb-fMRI, resting state fMRI (rsfMRI) is easy to apply because no task is executed. The functional relevance of rsfMRI has been proven as it measures intrinsic neuronal activities^{1, 5)}. Thus, rsfMRI has been extensively used to investigate brain disorders, such as Alzheimer's disease (AD)⁶⁻⁸⁾, autism spectrum disorder (ASD)⁹⁻¹¹⁾, and schizophrenia¹²⁻¹⁴⁾.

Most rsfMRI studies of brain disorders compare one or more functional metrics of rsfMRI such as functional connectivity between a group of patients with a group of normal subjects. Many studies have identified biomarkers discriminating the patient group from the normal group even by comparing measurements performed at different locations and with different scanners. Therefore, rsfMRI seems promising for investigating brain disorders.

The final goal of imaging brain disorder with rsfMRI is to detect or diagnose a brain disorder in an individual patient. However, it is challenging to apply data from group studies to individuals in particular because of the physical and physiological noises. Various methods, such as low or high-pass filters and independent component analysis, have been proposed to remove noises. Although those methods are effective, their performance to remove noises is not sufficient for using rsfMRI at the individual level.

In the present study, we attempted to remove noises using a new approach. We hypothesized that a set of physical noises originating from an MRI scanner and a set of physiological noises coming from a subject could be used as the basis of all the noises and could be removed from rsfMRI data. As proof of principle, we examined whether signals of one scan from a phantom model could be used to successfully remove signals in the following scans but also to remove noises from data acquired from a human subject.

Materials and Methods

Measurements of a phantom model and a human subject were performed. The human study was approved by the Institutional Review Board of the Tohoku Fukushi University (RS190607). One healthy volunteer participated in this study. MRI measurements were conducted using a 3-Tesla MRI scanner (Skyra-fit; Siemens) with a 20-channel matrix head coil. For rsfMRI measurements, the following parameters were used: repetition time = 1000 ms, echo time = 24 ms, matrix size = 64×64 , in-plane resolution = 3.4×3.4 mm², slice thickness = 3.4 mm, and number of volumes = 480. During the human rsfMRI scan, the subject was asked to lie on the bed with the eyes open, keeping his mind clear, and gently focusing the eyes on the center of the visual field. The lights in the room were turned off during the MRI scans.

Results and discussion

First, two MRI scan datasets from the phantom model were analyzed. Signals from phantom images were decomposed using the singular value decomposition method (SVD). Each first and second SVD components were derived from two MRI scans. Both components from the first scan were subtracted from the second scan. The subtraction reduced the first component value to almost zero but did not affect much the second component (Fig.1a, b). This suggested that regressing out SVD components of one scan from those of another scan in a one-to-one manner does not reduce much signal. To examine the correlation between both scans, maps of correlation between the SVD components of both scans were generated (Fig. 2). Many SVD components with high correlation values at off-diagonals were found. Because one SVD component of the first scan correlated with several SVD components of the second scan, we regressed out 10 components of the second scan from the first and second components of the first scan (Fig. 3). After regression, only a small amplitude residual signal of the first component was left, but the regression had almost no effect on the second component. Therefore, another regression was performed with more components (100 components). The amplitude of the residual signal from the second component was greatly reduced, by almost 10 times, after regression compared with that of the signal in Figure 3 b (Fig. 4). By regressing out 100 components, slow oscillations were removed from the first and the second components as shown in Figure 4. Therefore, a noise set acquired from a scan can be used as regressor to remove noises from another scan because all signals in the phantom model are noises and the reduction of signal amplitude and slow oscillations indicated that noises were removed. In addition, the reduction of the signals in Figure 4 suggested that MRI signals in both scans contain similar noises.

To apply the approach to the human brain, rsfMRI data were acquired with the same measurement parameters. Because we hypothesized that the physical noises made by the scanner in the phantom

model are the same that those measured with a human subject, the noise set (100 SVD components from the phantom data) was regressed from a time-course rsfMRI dataset acquired from a human subject. Figure 5 shows a human brain image acquired at the same slicing time as that at which the noise set was extracted in the phantom model. The time-course data from a voxel located in the occipital cortex were extracted (Fig. 5). After regressing the noise out, a residual signal of a much smaller amplitude than that from the original signal was left (Fig. 6). The remaining signal contained fewer band frequency components even compared with that of the band-pass filtered signal (0.01-0.15 Hz) (Fig. 6). Signal frequency spectrums, shown in Figure 7, were generated to examine the frequency characteristics of the remaining signals. The noise-depleted signal showed a narrower band than that of the band-pass filtered signal. Although the frequency components in the noise-depleted signal were narrower than those used in most rsfMRI studies, these results indicate that more reliable signals reflecting brain intrinsic functions can be obtained. To investigate functional aspects of the signal, the signal was used as seed to generate a correlation map, shown in Figure 8. The pattern of the correlation map obtained using the noise-regressed signal was similar to the one obtained using the band-pass filtered signal. The hot voxels on the correlation map obtained with the noise-regressed signal were less spread (Fig. 8). This suggested that the noise-regressed signal contained meaningful functional components compatible with those found in the band-passed signal and provided more specific functional information. Future studies including more human subject data and devising more regression models are expected to confirm the results of the present preliminary work.

In conclusion, we showed that noise-free intrinsic functional signals were obtained from rsfMRI data by using previously prepared sets of physical and physiological noises as regressors in conditions where noises are restricted to the scanner and subject environments.

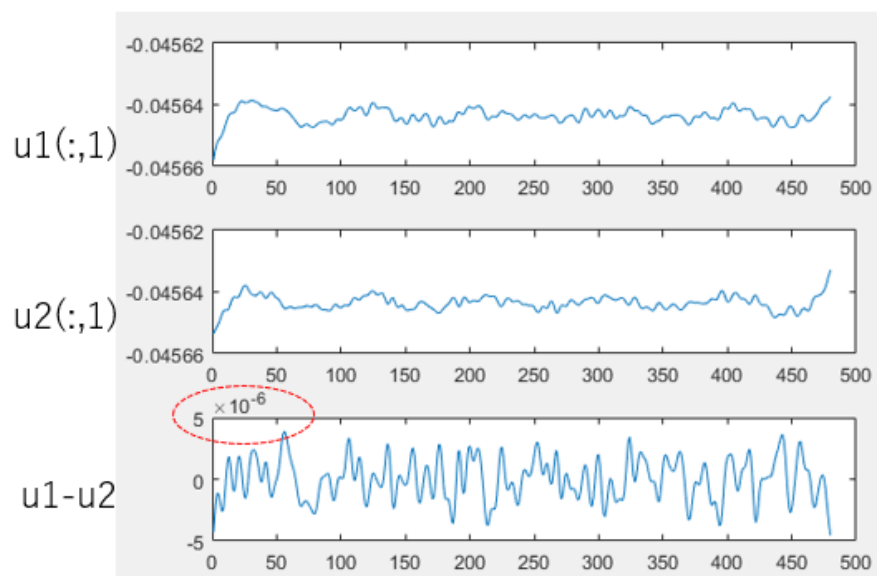


Figure 1 a. First SVD components of the first (top panel) and the second (middle panel) scans. The signal amplitude was very small after subtraction of both components (bottom panel). The horizontal axis represents the time in seconds. The vertical axis represents arbitrary values. The characters $u1(:,1)$ stand for the first SVD component of the first scan and $u2(:,1)$ stands for the first SVD component of the second scan.

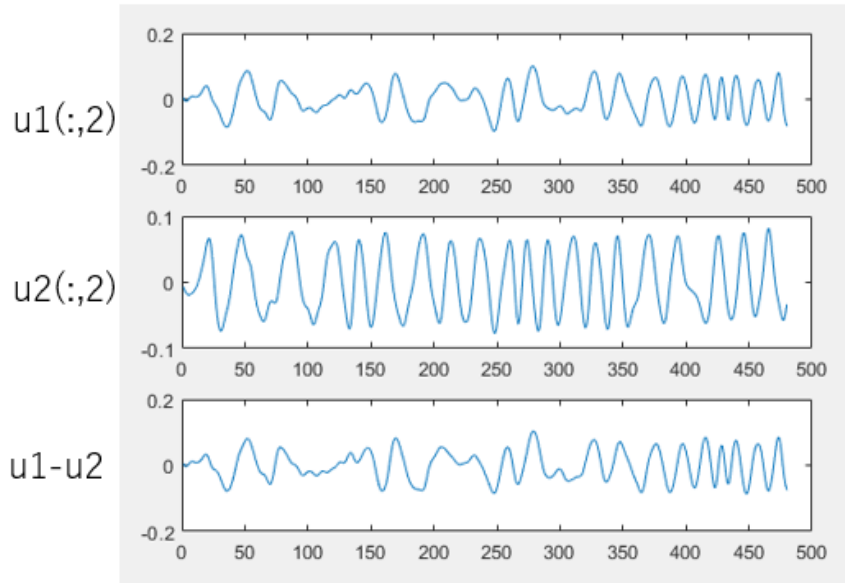


Figure 1 b. Second SVD components of the first scan (top panel) and the second scan (middle panel). The subtraction of the two components leaves a signal with a very small amplitude (bottom panel). The horizontal axis represents time in second. The vertical axis represents arbitrary values. The character $u1(:,2)$ stands for the second SVD component of the first scan, $u2(:,2)$ stands for the second SVD component of the second scan.

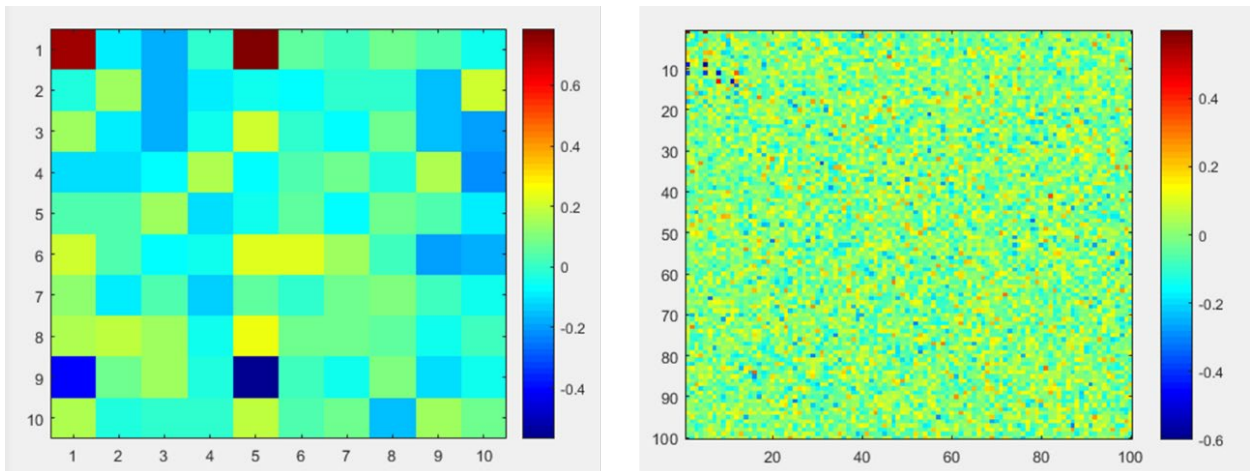


Figure 2. Correlation maps between SVD components from two scans. The left is correlation map for 10 components and the right is correlation map for 100 components.

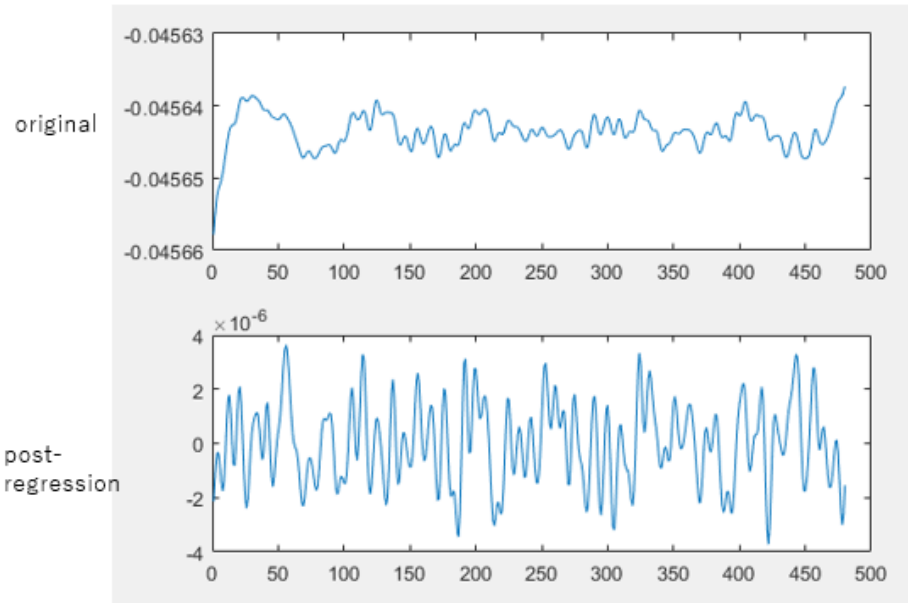


Figure 3 a. First component signal of the first scan (upper panel) and the residual signal after the regression of 10 components in the second scan (bottom panel). Only a small amplitude signal was left after the regression.

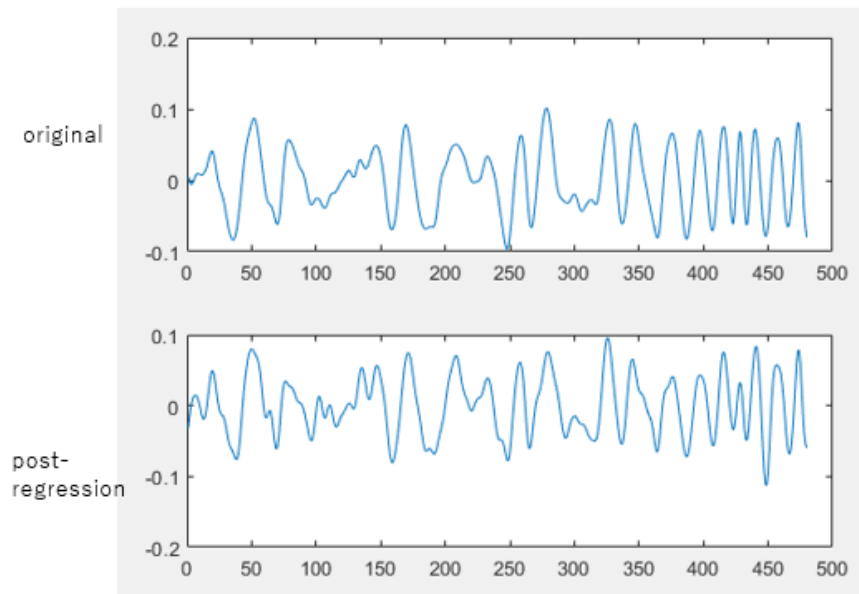


Figure 3 b. Second component of the first scan (upper panel) and the residual signal after the regression of 10 components in the second scan (bottom panel). The residual signal is not much different from the original component.

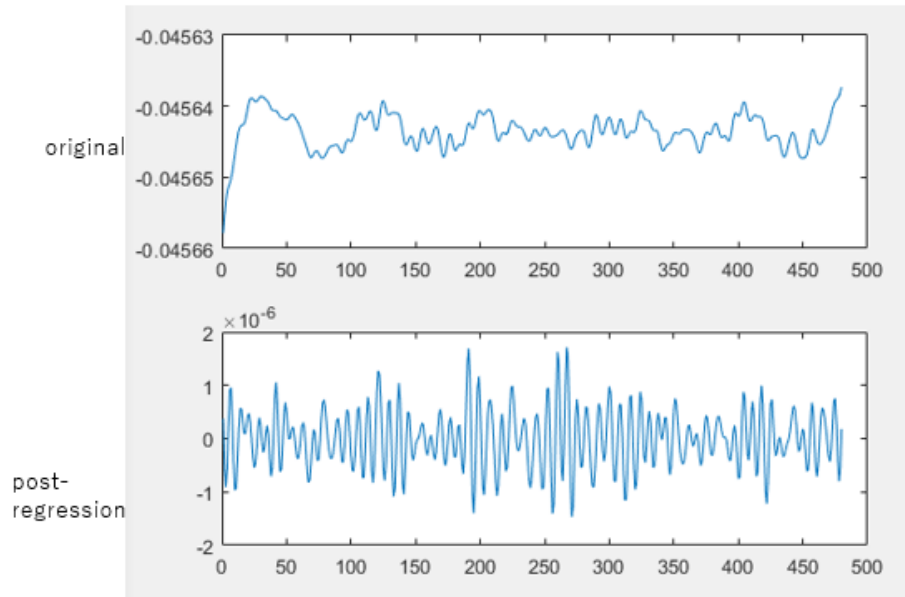


Figure 4 a. First component of the first scan (upper panel) and the residual signal after the regression of 100 components in the second scan (bottom panel). Only a small amplitude signal was left after the regression. The amplitude of the residual signal was a little more reduced and the slow oscillation was much more reduced.

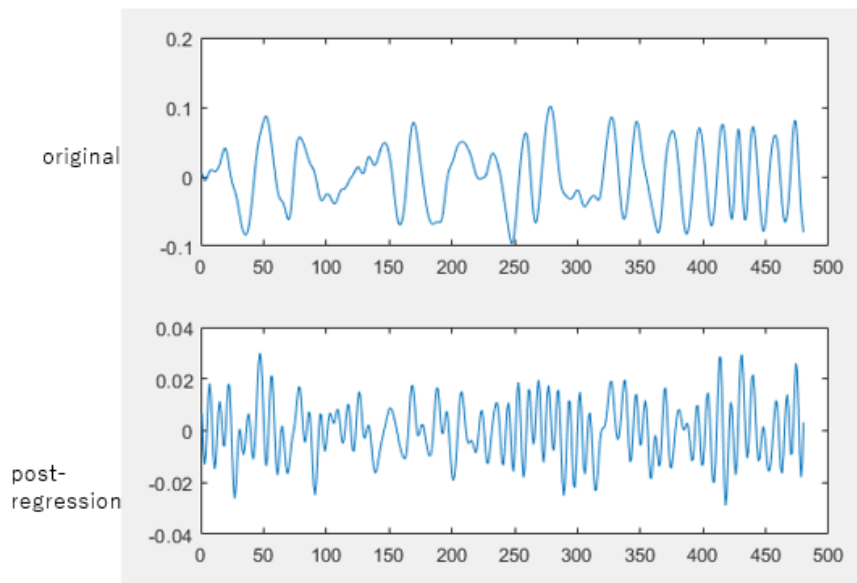


Figure 4 b. Second component of the first scan (upper panel) and the residual signal after the regression of 100 components in the second scan (bottom panel). The amplitude of the residual signal is much reduced in comparison with the regression of 10 components with slow oscillation reduction.

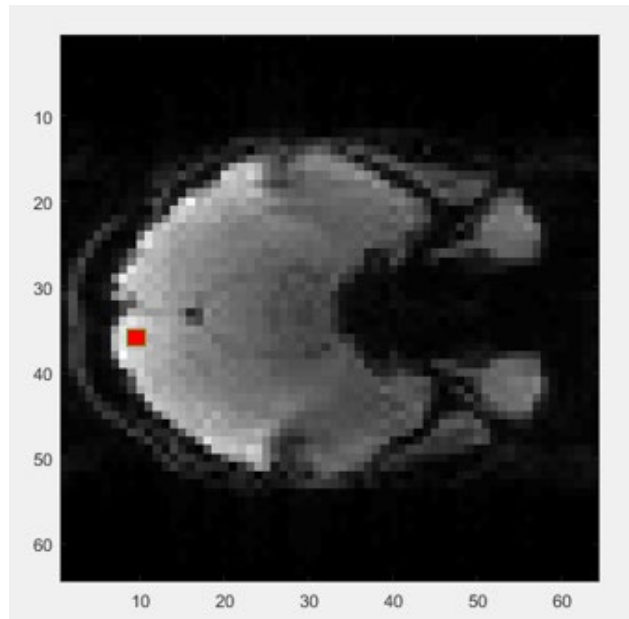


Figure 5. An image slice of the human subject. Time-course was extracted from the small red rectangular. The location is corresponding to the occipital cortex.

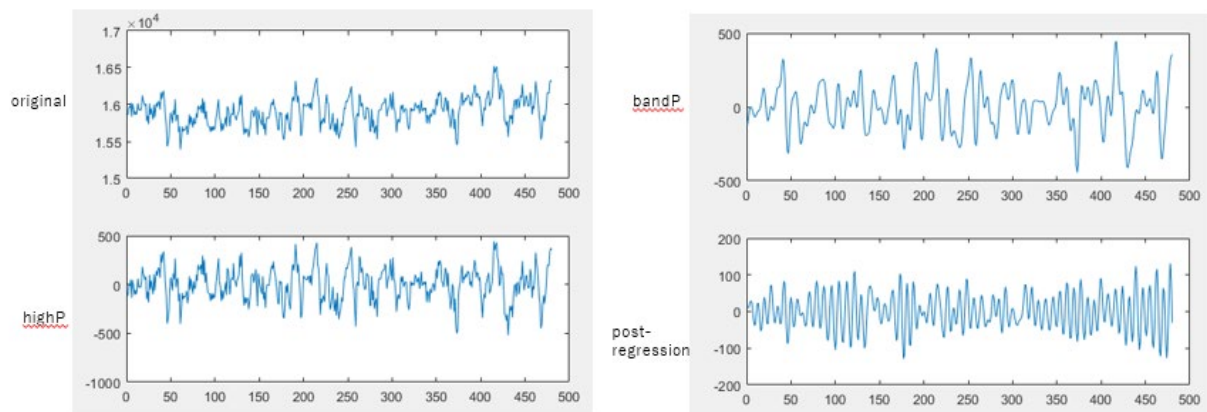


Figure 6. Original (upper-left), high-pass filtered (lower-left), band-pass filtered (upper-right), and noise-regressed (lower-right) signals.

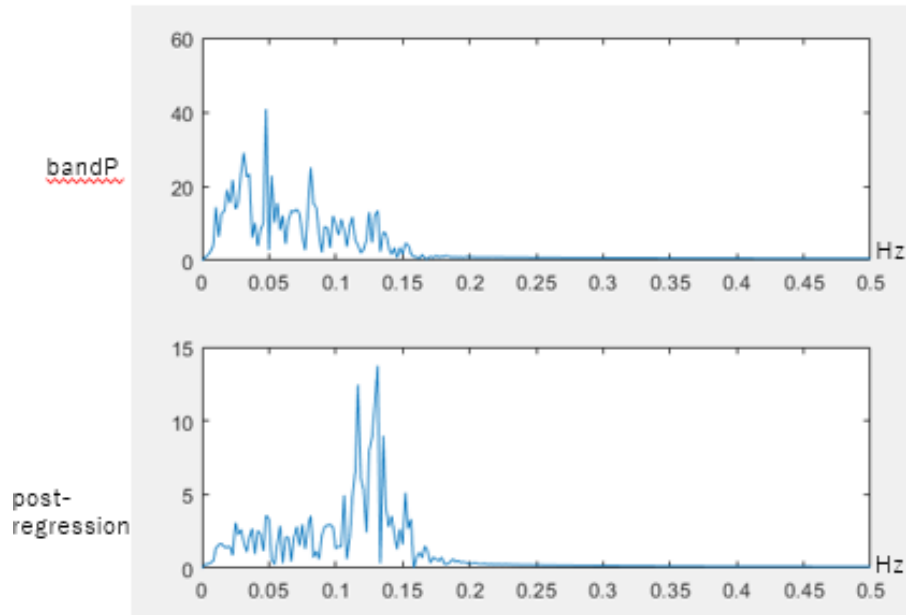


Figure 7. Frequency spectrums of band-passed filtered and noise-regressed signals.

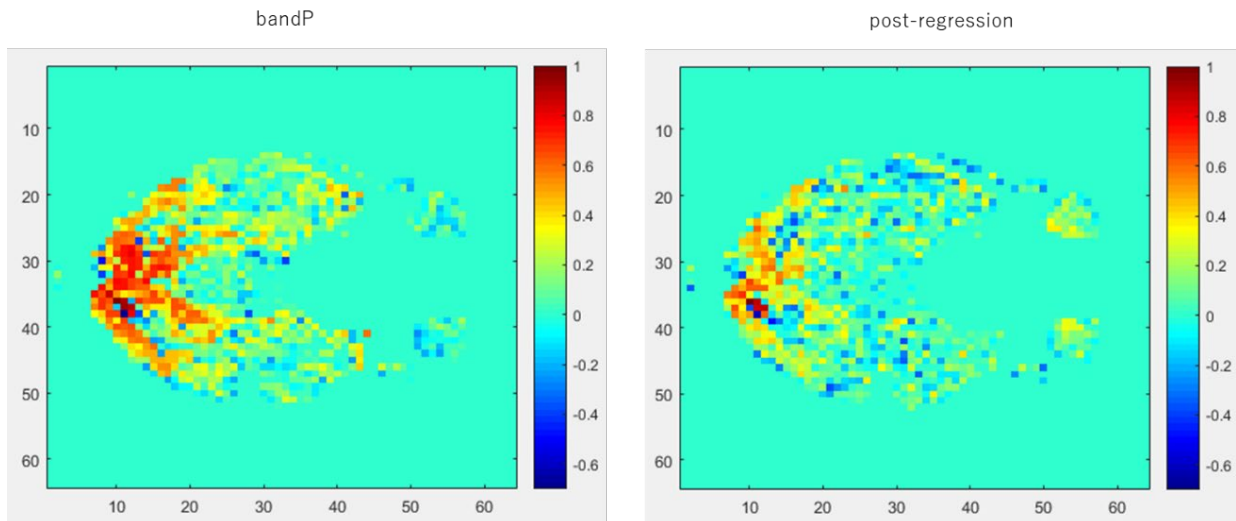


Figure 8. Correlation maps used band-passed signal (left) and noise-regressed signal (right) as the seed. Color bar stands for correlation values.

Acknowledgement

This study was carried out as a part of the cooperative research project at the Kansei Research Institute of Tohoku Fukushi University, receiving a subsidy of the research facility operation support MEXT, and JSPS KAKENHI Grant Number 21H02800 & 19H00532 & 19H01111.

References

- 1) Biswal B, Van Kylen J, Hyde JS. (1997) Simultaneous assessment of flow and BOLD signals in resting-state functional connectivity maps. *NMR Biomed.* 1997 Jun-Aug;10 (4-5) :165-170.

- 2) Biswal B, Yetkin FZ, Haughton VM, Hyde JS. (1995) Functional connectivity in the motor cortex of resting human brain using echo-planar MRI. *Magn Reson Med* 10: 537-141.
- 3) Damoiseaux JS, Rombouts SA, Barkhof F, Scheltens P, Stam CJ, Smith SM, Beckmann CF. (2006) Consistent resting-state networks across healthy subjects. *Proc. Natl. Acad. Sci. U. S. A.*, 103: 13848-13853
- 4) Fransson P. (2005) Spontaneous low-frequency BOLD signal fluctuations: an fMRI investigation of the resting-state default mode of brain function hypothesis. *Hum. Brain Mapp.* 26: 15-29.
- 5) Fox MD, Corbetta M, Snyder AZ, Vincent JL, Raichle ME. (2006) Spontaneous neuronal activity distinguishes human dorsal and ventral attention systems. *PNAS* 103: 10046-10051.
- 6) Göttler J, Preibisch C, Riederer I, Pasquini L, Alexopoulos P, Bohn KP, Yakushev I, Beller E, Kaczmarz S, Zimmer C, Grimmer T, Drzezga A, Sorg C. (2018) Reduced blood oxygenation level dependent connectivity is related to hypoperfusion in Alzheimer's disease. *J Cereb Blood Flow Metab.* 2018 Jan 1 :271678X18759182. doi: 10.1177/0271678X18759182.
- 7) Wang B, Niu Y, Miao L, Cao R, Yan P, Guo H, Li D, Guo Y, Yan T, Wu J, Xiang J, Zhang H. (2018) Decreased Complexity in Alzheimer's Disease: Resting-State fMRI Evidence of Brain Entropy Mapping. *Front Aging Neurosci.* 2017 Nov 20; 9 :378. doi: 10.3389/fnagi.2017.00378.
- 8) Zhang J, Guo Z, Liu X, Jia X, Li J, Li Y, Lv D, Chen W. (2017) Abnormal functional connectivity of the posterior cingulate cortex is associated with depressive symptoms in patients with Alzheimer's disease. *Neuropsychiatr Dis Treat.* 13, 2589-2598.
- 9) Jack A. (2018) Neuroimaging in neurodevelopmental disorders: focus on resting-state fMRI analysis of intrinsic functional brain connectivity. *Curr Opin Neurol.* doi: 10.1097/WCO.0000000000000536.
- 10) Duan X, Chen H, He C, Long Z, Guo X, Zhou Y, Uddin LQ, Chen H. (2017) Resting-state functional under-connectivity within and between large-scale cortical networks across three low-frequency bands in adolescents with autism. *Prog Neuropsychopharmacol Biol Psychiatry* 79, 434-441.
- 11) Hegarty JP 2nd, Ferguson BJ, Zamzow RM, Rohowetz LJ, Johnson JD, Christ SE, Beversdorf DQ. (2017) Beta-adrenergic antagonism modulates functional connectivity in the default mode network of individuals with and without autism spectrum disorder. *Brain Imaging Behav* 11, 1278-1289.
- 12) Huang H, Shu C, Chen J, Zou J, Chen C, Wu S, Xiao L, Liu Z, Wang H, Zhou Y, Wang G, Jiang T. (2018) Altered corticostriatal pathway in first-episode paranoid schizophrenia: Resting-state functional and causal connectivity analyses. *Psychiatry Res.* 272, 38-45.
- 13) Wang S, Zhan Y, Zhang Y, Lyu L, Lyu H, Wang G, Wu R, Zhao J, Guo W. (2018) Abnormal long- and short-range functional connectivity in adolescent-onset schizophrenia patients: A resting-state fMRI study. *Prog Neuropsychopharmacol Biol Psychiatry* 81, 445-451.
- 14) Sharma A, Kumar A, Singh S, Bhatia T, Beniwal RP, Khushu S, Prasad KM, Deshpande SN. (2018) Altered resting state functional connectivity in early course schizophrenia. *Psychiatry Res.* 271,17-23.